Supplementary materials

The cif files are for the single-crystal structure refinements for the five coesite samples (R503, R663, R694, R712 and R749).

Appendix Table 1. Anisotropic displacement parameters *(*Å^2) for the synthetic coesite samples in this study.

		R503	R663	R694	R712	R749
Si1	U_{11}**:**	0.0066 (5)	0.0055 (5)	0.0051 (4)	0.0077 (4)	0.0073 (5)
	U_{22}**:**	0.0076 (6)	0.0072 (5)	0.0034 (4)	0.0083 (5)	0.0047 (4)
	U_{33}**:**	0.0074 (4)	0.0102 (7)	0.0048 (4)	0.0078 (4)	0.0086 (5)
	U_{12}**:**	-0.0014 (3)	-0.0009 (3)	-0.00095 (17)	-0.0012 (2)	-0.0014 (2)
	U_{13}**:**	0.0043 (4)	0.0044 (5)	0.0026 (3)	0.0030 (4)	0.0043 (4)
	U_{23}**:**	-0.0008 (3)	-0.0007 (3)	-0.00062 (17)	-0.0007 (2)	-0.0009 (2)
	U_{eq}**:**	0.0069 (3)	0.0074 (4)	0.0043 (3)	0.0083 (3)	0.0067 (3)
Si2	U_{11}**:**	0.0066 (5)	0.0053 (5)	0.0056 (4)	0.0083 (4)	0.0075 (5)
	U_{22}**:**	0.0075 (5)	0.0072 (5)	0.0034 (4)	0.0084 (4)	0.0049 (4)
	U_{33}**:**	0.0063 (4)	0.0098 (7)	0.0043 (4)	0.0073 (4)	0.0075 (6)
	U_{12}**:**	-0.0001 (3)	-0.0003 (2)	-0.00013 (17)	-0.0002 (2)	-0.0001 (2)
	U_{13}**:**	0.0038 (4)	0.0041 (4)	0.0029 (3)	0.0035 (3)	0.0040 (4)
	U_{23}**:**	0.0001 (3)	0.0000 (3)	-0.00005 (17)	-0.0003 (2)	-0.0001 (2)
	U_{eq}**:**	0.0065 (3)	0.0073 (4)	0.0043 (3)	0.0082 (3)	0.0066 (3)

O1	U_{11}:	0.0091 (15)	0.0084 (15)	0.0094 (11)	0.0108 (12)	0.0114 (14)
	U_{22}:	0.0070 (18)	0.0087 (14)	0.0044 (7)	0.0086 (13)	0.0053 (12)
	U_{33}:	0.0127 (11)	0.015 (2)	0.0097 (10)	0.0117 (12)	0.0130 (15)
	U_{12}:	-0.0034 (12)	-0.0018 (10)	-0.0026 (7)	-0.0024 (9)	-0.0022 (8)
	U_{13}:	0.0051 (12)	0.0069 (16)	0.0044 (9)	0.0035 (11)	0.0060 (14)
	U_{23}:	-0.0013 (12)	-0.0002 (11)	-0.0011 (8)	-0.0017 (10)	-0.0004 (9)
	U_{eq}:	0.0098 (7)	0.0101 (7)	0.0080 (5)	0.0113 (6)	0.0100 (6)
O2	U_{11}:	0.0112 (15)	0.0101 (16)	0.0091 (11)	0.0123 (10)	0.0111 (14)
	U_{22}:	0.0133 (18)	0.0100 (13)	0.0074 (10)	0.0113 (13)	0.0087 (12)
	U_{33}:	0.0081 (11)	0.014 (2)	0.0056 (11)	0.0078 (12)	0.0094 (15)
	U_{12}:	0	0	0	0	0
	U_{13}:	0.0065 (12)	0.0086 (17)	0.0040 (10)	0.0052 (12)	0.0057 (13)
	U_{23}:	0	0	0	0	0
	U_{eq}:	0.0101 (7)	0.0101 (8)	0.0072 (5)	0.0103 (6)	0.0094 (6)
O3	U_{11}:	0.0098 (11)	0.0099 (11)	0.0100 (9)	0.0108 (9)	0.0099 (10)
	U_{22}:	0.0111 (13)	0.0144 (10)	0.0094 (7)	0.0139 (10)	0.0107 (9)
	U_{33}:	0.0126 (9)	0.0180 (16)	0.0102 (8)	0.0121 (9)	0.0145 (11)
	U_{12}:	0.0017 (9)	0.0028 (7)	0.0019 (5)	0.0017 (7)	0.0022 (6)
	U_{13}:	0.0077 (9)	0.0099 (12)	0.0077 (7)	0.0062 (9)	0.0082 (9)

	U_{23}:	0.0013 (8)	0.0015 (8)	0.0011 (5)	0.0014 (7)	0.0009 (6)
	U_{eq}:	0.0102 (5)	0.0128 (6)	0.0086 (4)	0.0121 (5)	0.0108 (5)
O4	U_{11}:	0.0117 (11)	0.0122 (11)	0.0105 (9)	0.0123 (10)	0.0124 (10)
	U_{22}:	0.0121 (13)	0.0134 (10)	0.0089 (7)	0.0155 (10)	0.0101 (9)
	U_{33}:	0.0084 (9)	0.0128 (16)	0.0055 (8)	0.0088 (9)	0.0102 (13)
	U_{12}:	-0.0016 (10)	-0.0024 (8)	-0.0022 (5)	-0.0028 (7)	-0.0031 (6)
	U_{13}:	0.0039 (9)	0.0050 (11)	0.0014 (7)	0.0029 (9)	0.0040 (10)
	U_{23}:	-0.0014 (8)	-0.0009 (8)	-0.0014 (5)	-0.0020 (7)	-0.0023 (6)
	U_{eq}:	0.0113 (5)	0.0134 (6)	0.0094 (4)	0.0133 (5)	0.0116 (5)
O5	U_{11}:	0.0128 (11)	0.0087 (12)	0.0094 (9)	0.0129 (10)	0.0116 (11)
	U_{22}:	0.0075 (14)	0.0088 (10)	0.0036 (7)	0.0086 (9)	0.0054 (8)
	U_{33}:	0.0151 (9)	0.0166 (17)	0.0129 (9)	0.0153 (9)	0.0139 (12)
	U_{12}:	-0.0012 (10)	0.0004 (7)	0.0005 (5)	-0.0001 (7)	-0.0008 (6)
	U_{13}:	0.0094 (9)	0.0073 (12)	0.0064 (7)	0.0072 (8)	0.0072 (10)
	U_{23}:	-0.0009 (8)	-0.0003 (7)	0.0001 (5)	-0.0001 (7)	-0.0005 (6)
	U_{eq}:	0.0108 (5)	0.0109 (6)	0.0083 (4)	0.0123 (5)	0.0100 (5)

Appendix Table 2. The frequencies of the Raman-active modes at ambient condition, as well as the temperature dependence and γ_{iP} parameters.

	R503			**R663**			**R712**			**R749**	
v_i (cm^{-1})	$(\delta v_i/\delta T)_p$ ($cm^{-1}\cdot K^{-1}$)	γ_{iP}	v_i (cm^{-1})	$(\delta v_i/\delta T)_p$ ($cm^{1}\cdot K^{-1}$)	γ_{iP}	v_i (cm^{-1})	$(\delta v_i/\delta T)_p$ ($cm^{1}\cdot K^{-1}$)	γ_{iP}	v_i (cm^{-1})	$(\delta v_i/\delta T)_p$ ($cm^{-1}\cdot K^{-1}$)	γ_{iP}
1166	-0.0145(12)	1.48(12)	1168	-0.0261(18)	2.66(18)	1170	-0.0275(13)	2.79(13)	—	—	—
1148	-0.0309(11)	3.20(11)	1149	-0.0147(16)	1.52(17)	1051	-0.0277(9)	3.13(10)	—	—	—
1041	-0.0229(4)	2.61(4)	1041	-0.0238(6)	2.72(7)	1044	-0.0231(8)	2.63(9)	1038	-0.0201(5)	2.30(6)
817	-0.0174(4)	2.53(5)	818	-0.0125(9)	1.81(13)	820	-0.0161(2)	2.33(3)	—	—	—
787	-0.0241(20)	3.64(30)	789	-0.0113(3)	1.70(5)	791	-0.0135(3)	2.03(5)	784	-0.0110(8)	1.67(12)
—	—	—	663	0.0012(1)	-0.21(2)	649	-0.0209(6)	3.83(11)	698	-0.0125(7)	2.13(11)
521	-0.0065(2)	1.48(4)	523	-0.0076(2)	1.72(4)	522	-0.0058(1)	1.32(2)	523	-0.0059(1)	1.34(2)
467	-0.0063(4)	1.60(10)	469	-0.0061(20)	1.54(50)	468	-0.0068(2)	1.72(5)	468	-0.0045 (6)	1.14(15)
428	-0.0036(11)	1.00(30)	429	-0.0025(2)	0.69(5)	428	-0.0001(1)	0.02(2)	430	-0.0015(2)	0.41(5)
—	—	—	—	—	—	381	-0.0133(9)	4.15(28)	379	-0.0074(6)	2.32(18)
356	-0.0043(2)	1.43(6)	357	-0.0039(2)	1.30(6)	357	-0.0020(1)	0.66(3)	—	—	—
326	-0.0101(7)	3.68(25)	328	-0.0070(7)	2.54(25)	327	-0.0041(1)	1.49(3)	326	-0.0025(8)	0.91(29)
271	-0.0037(5)	1.63(21)	273	-0.0049(2)	2.13(8)	272	-0.0030(1)	1.31(3)	270	-0.0019(1)	0.83(4)
246	-0.0092(9)	4.45(43)	248	-0.0110(28)	5.28(134)	—	—	—	—	—	—
229	0.0068(25)	-3.53(129)	231	-0.0003(9)	0.15(46)	—	—	—	—	—	—
205	-0.0059(4)	3.42(23)	207	-0.0058(5)	3.33(28)	206	-0.0042(3)	2.42(17)	204	-0.0046(2)	2.68(11)
178	-0.0149(6)	9.96(40)	180	-0.0095(8)	6.28(52)	179	-0.0065(5)	4.32(33)	177	-0.0082(5)	5.51(33)
151	-0.0150(15)	11.82(118)	154	-0.0015(11)	1.15(85)	152	0.0026(2)	-2.03(15)	151	0.0075(11)	-5.91(86)
119	-0.0209(15)	20.90(150)	121	-0.0226(14)	22.23(137)	120	-0.0185(14)	18.35(138)	117	-0.0180(12)	18.31(122)
79	-0.0105(9)	15.82(135)	—	—	—	—	—	—	—	—	—

Appendix Table 3. The frequencies of the OH bands by FTIR measurement at ambient temperature if not noted, as well as their temperature dependence.

R503		**R663**		**R694**		**R749**	
v_i (cm^{-1})	$(\delta v_i/\delta T)_p$ ($cm^{-1}\cdot K^{-1}$)	v_i (cm^{-1})	$(\delta v_i/\delta T)_p$ ($cm^{1}\cdot K^{-1}$)	v_i (cm^{-1})	$(\delta v_i/\delta T)_p$ ($cm^{1}\cdot K^{-1}$)	v_i (cm^{-1})	$(\delta v_i/\delta T)_p$ ($cm^{-1}\cdot K^{-1}$)
3300	0.1663	3300	0.0612	3300	0.1372	3300	0.0402
3458	0.1251	3458	0.0588	3458	0.1112	3458	0.1610
—	—	3500	0.0148	3500	0.0201	—	—
3522	0.0074	3523	0.0142	3523	0.0189	3522	0.0562
3540[a]	0.0069	3538[a]	0.0087	3526[a]	0.0576	3510[a]	0.0558
3572	-0.1553	3572	-0.1976	3572	-0.1005	3568	-0.0798

a: the maximum positions for the broad humps at high temperatures around 600 K.

Supplementary Figures:

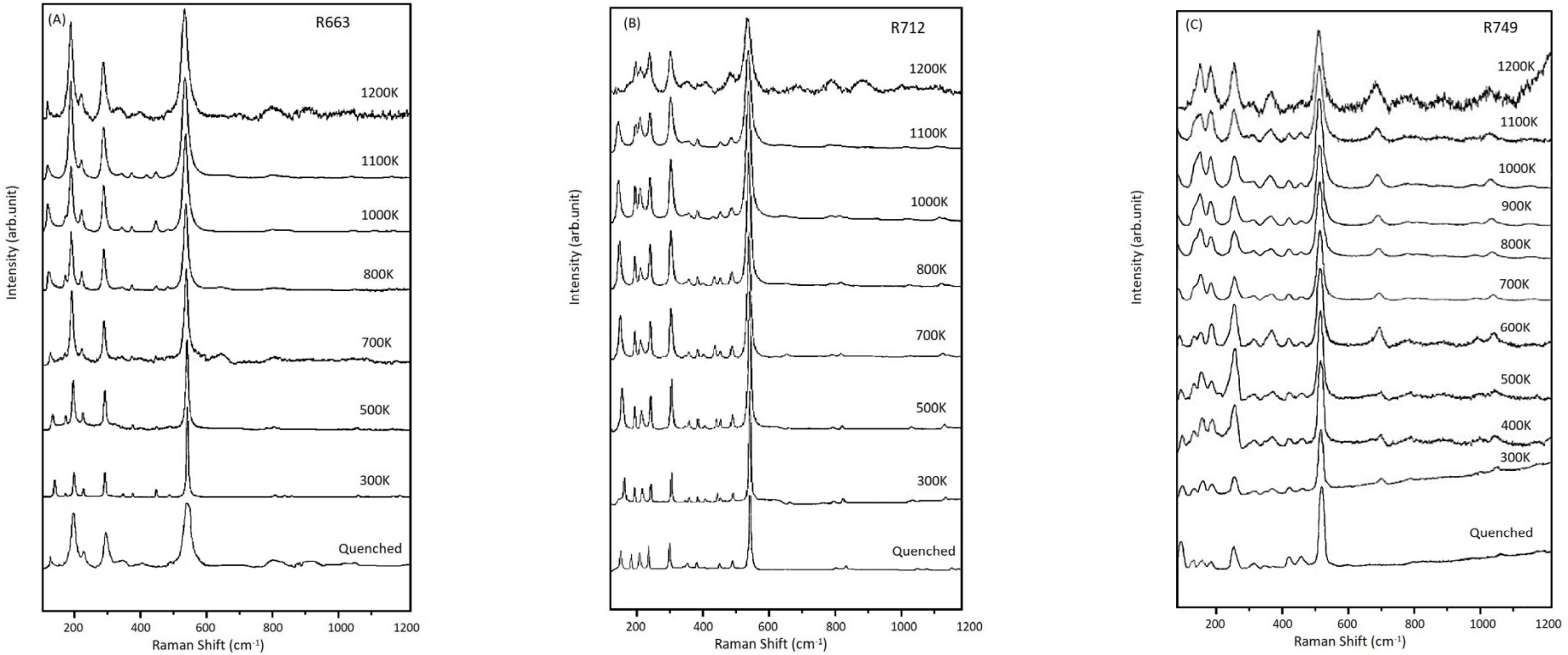

Figure S1. Selected high-temperature Raman spectra as well as the pattern taken when quenched to room temperature for the samples of **(A)** R663, **(B)** R712 and **(C)** R749.

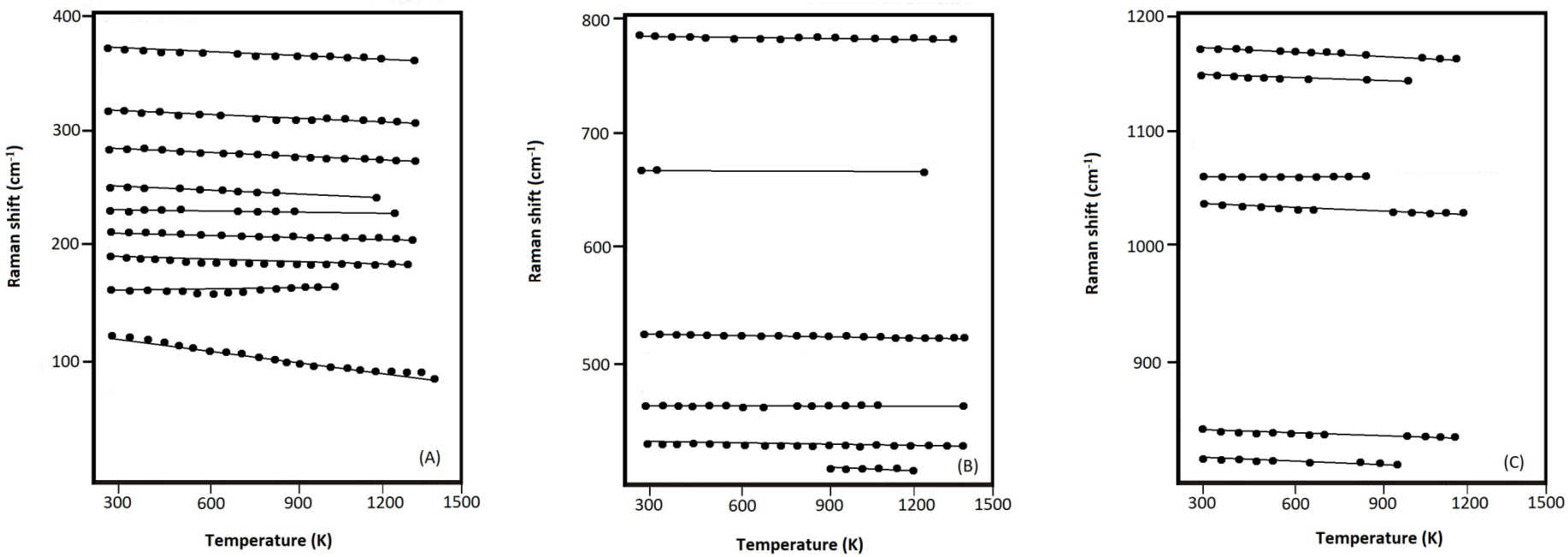

Figure S2. The frequencies for the Raman-active modes as a function of temperature for the sample of ***R712***: **(A)** 0 - 400 cm^{-1}, **(B)** 400 - 800 cm^{-1} and **(C)** 800 - 1200 cm^{-1}. Linear regression is fitted for each dataset.

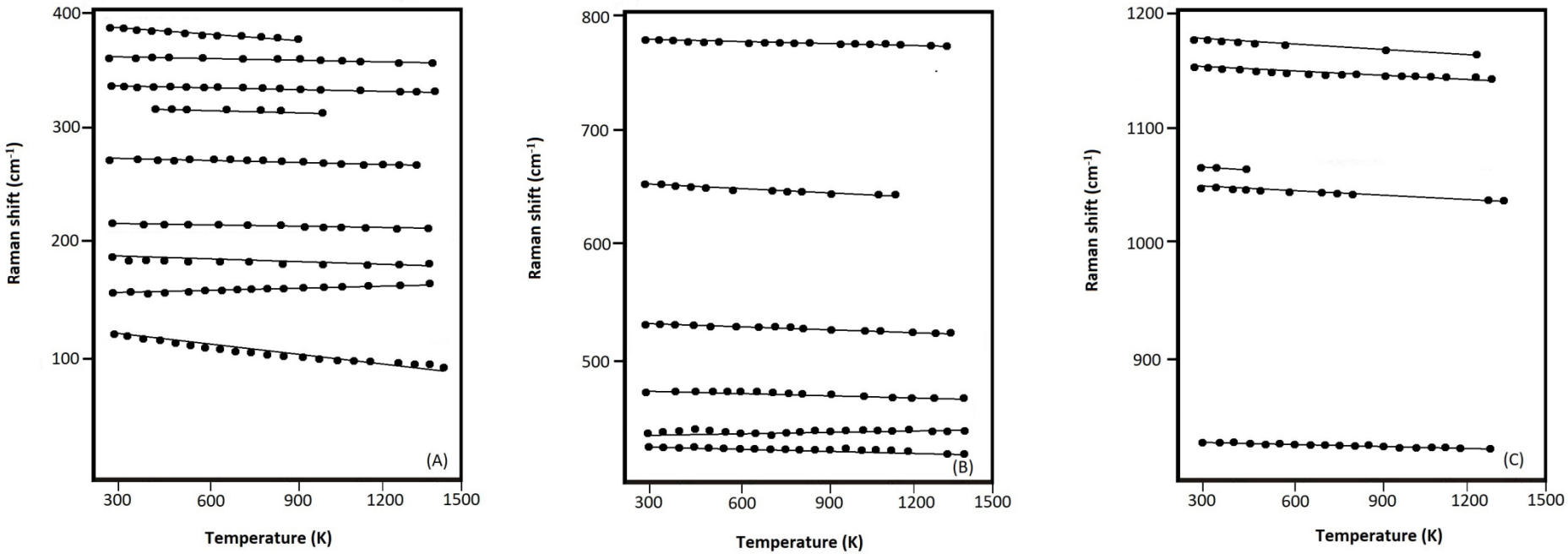

Figure S3. The frequencies for the Raman-active modes as a function of temperature for the sample of ***R663***: **(A)** 0 - 400 cm^{-1}, **(B)** 400 - 800 cm^{-1} and **(C)** 800 - 1200 cm^{-1}. Linear regression is fitted for each dataset.

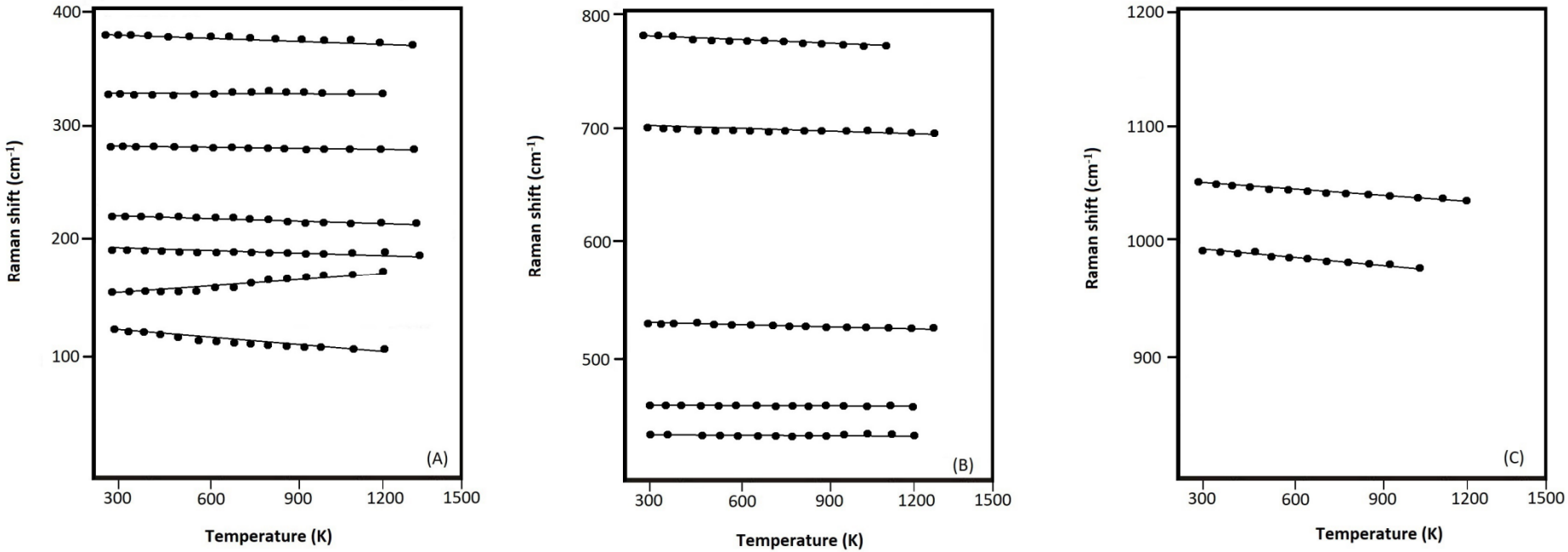

Figure S4. The frequencies for the Raman-active modes as a function of temperature for the sample of ***R749***: **(A)** 0 - 400 cm^{-1}, **(B)** 400 - 800 cm^{-1} and **(C)** 800 - 1200 cm^{-1}. Linear regression is fitted for each dataset.

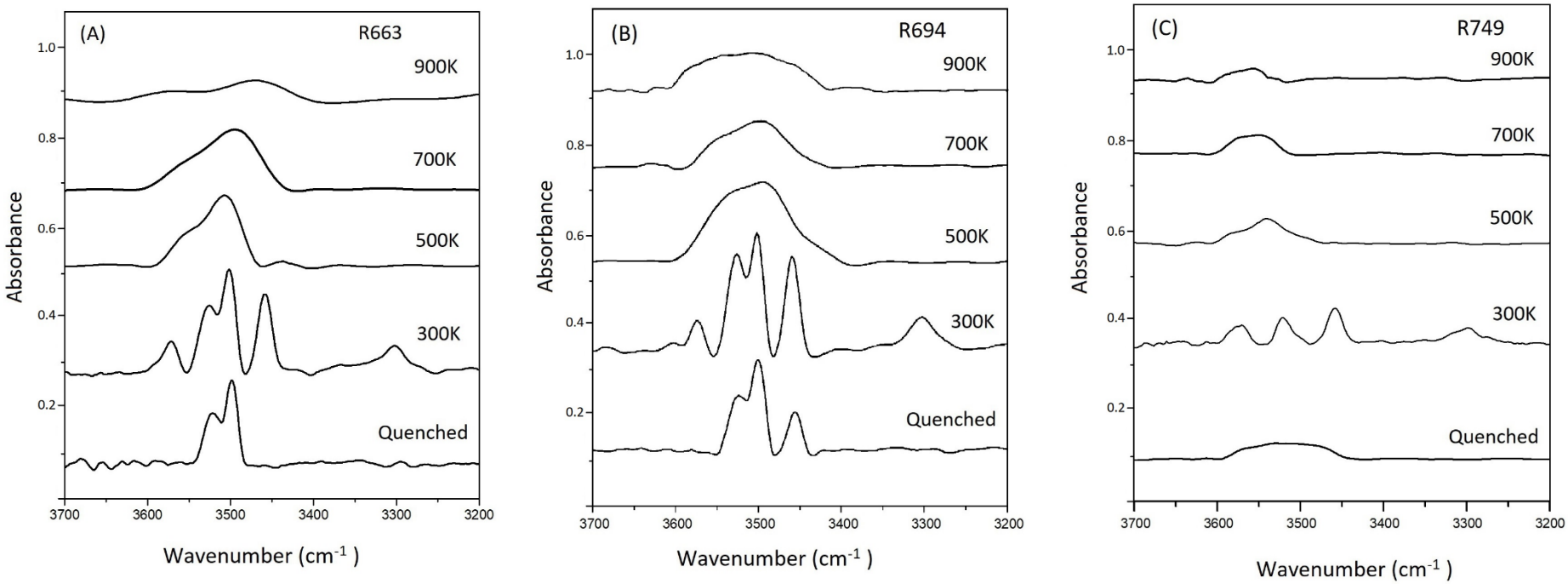

Figure S5. Representative FTIR spectra obtained at high temperatures as well as when quenched to room temperature for the samples of **(A)** R663, **(B)** R694 and **(C)** R749.